The production of diverse brGDGTs by an Acidobacterium allows a direct test of temperature and pH controls on their distribution

Yufei Chen[a,b,1], Fengfeng Zheng[a,b,1], Huan Yang[c,1], Wei Yang[a], Ruijie Wu[a], Xinyu Liu[a], Huayang Liang[a], Huahui Chen[a], Hongye Pei[c], Chuanlun Zhang[a,b,d], Richard D. Pancost[e], Zhirui Zeng[a,b,*]

[a]Department of Ocean Science and Engineering, Southern University of Science and Technology, Shenzhen 518055, China

[b]Southern Marine Science and Engineering Guangdong Laboratory (Guangzhou), Guangzhou, 511458, China

[c]State Key Laboratory of Biogeology and Environmental Geology, Hubei Key Laboratory of Critical Zone Evolution, School of Geography and Information Engineering, China University of Geosciences, Wuhan, 430074, China

[d]Shenzhen Key Laboratory of Marine Archaea Geo-Omics, Southern University of Science and Technology, Shenzhen 518055, China

[e]Organic Geochemistry Unit, School of Chemistry, School of Earth Sciences, Cabot Institute for the Environment, University of Bristol, Cantock's Close, Bristol BS8 1TS, UK

[1]Y.C., F.Z. and H.Y. contributed equally to this work.

22 PHYSICAL SCIENCES: Earth, Atmospheric, and Planetary Sciences

23 BIOLOGICAL SCIENCES: Microbiology

24

25 Corresponding Author

26 Zhirui Zeng, Department of Ocean Science and Engineering, Southern University of

27 Science and Technology, Shenzhen 518055, China, zengzr@sustech.edu.cn

28

29 Keywords: brGDGTs, Acidobacteria, lipid biomarker, membrane adaption,

30 paleoclimate proxies

31

Abstract

Microbial lipid biomarkers preserved in geological archives can be used to explore past climate changes. Branched glycerol dialkyl glycerol tetraethers (brGDGTs) are unique bacterial biomarkers that have been used as molecular tools for the quantitative determination of terrestrial temperatures and the pH of depositional environments over a range of geological timescales. However, the exact biological source organisms – especially of the entire suite of brGDGTs found in the environment – remains unclear; by extension, so do the mechanisms that govern these proxies. Here, we identified a brGDGT-producing strain *Candidatus Solibacter usitatus* Ellin6076, by identifying archaeal tetraether synthase homologs in bacterial genomes. This strain synthesizes diverse brGDGTs, including regular C_5-methylated and cyclic brGDGTs, and brGDGTs comprise up to 66% of the major lipids, far exceeding the proportions found in previous studies. The degree of C_5-methylation in cultured strain Ellin6076 is primarily determined by temperature, whereas cyclization appears to be influenced by multiple factors. Consequently, culture-derived paleoclimate indices are in agreement with the global soil-derived MBT'$_{5ME}$ (methylation index of C_5-methyl brGDGTs) proxy for temperature but not the CBT$_{5ME}$ (cyclization index of C_5-methyl brGDGTs) proxy for pH. Our findings provide important insights from a physiological perspective into the underlying mechanism of brGDGT-based proxies.

Significance Statement

Branched glycerol dialkyl glycerol tetraethers (brGDGTs) are biomarkers widely used for the quantitative estimation of past climatic changes due to their ubiquitous occurrence in the environment and the relationships between their distributions and temperature and pH. However, the ecophysiology of brGDGT-producing bacteria and the mechanistic basis for brGDGT-based climate proxies remain unknown. Here, we identify a brGDGT-producing Acidobacterium and present a physiological study of brGDGTs in response to cultivation variables, which provides pivotal insights into how brGDGT producers modulate methylation and cyclization under different culturing conditions. Our study represents a significant advancement in understanding the physiological role of lipid structures in microbial adaptation and helps us interpret the relationships between brGDGT-based proxies and environmental conditions of the geological environment.

Introduction

Quantitative estimation of past climate change is important for understanding Earth history, contextualising the impact of recent human-induced climate change, and testing models used for future projections. This is challenging, particularly for the terrestrial environment, due to the scarcity of quantitative proxies for the reconstruction of climate variables, e.g. temperature and precipitation. Microbial lipid biomarkers preserved in terrestrial climate archives offer several useful tools for documenting the evolution of Earth's climate (1). Branched glycerol dialkyl glycerol tetraethers (brGDGTs) are one class of such lipids and have been used to reconstruct past temperature, paleohydrology, pH, and terrigenous organic input (2–5). Due to their ubiquitous occurrence in terrestrial and aquatic settings, the number of their applications to climate archives, e.g. paleosols, peats, lake sediments, stalagmites, estuarine and marine sediments, has increased dramatically over the last decade (3, 6).

These applications rest on the empirical relationships between the distribution of brGDGTs and environmental variables, such as temperature, mean annual precipitation, and pH in modern soils and surface sediments (7–9). In particular, considerable efforts have been devoted to improving our understanding and the accuracy of brGDGT-based temperature or pH proxies (2, 10, 11). However, uncertainties persist, many arising from the fact that the microbial producers of these mysterious lipids in the environment remain incomplete (12, 13). This has prevented an examination of the ecophysiology of these microbes and testing of these proxies under laboratory conditions.

87 The quest for the microbial producer(s) of brGDGTs has been ongoing since the
88 discovery of brGDGTs almost twenty years ago (14). The enantiomeric configuration
89 of the glycerol backbone, 1,2-di-*O*-alkyl-*sn*-glycerol, assigns brGDGTs as lipids that
90 are synthesized by bacteria (15). A paired 16S rRNA gene sequencing and brGDGT
91 approach was used in numerous studies to help constrain the identity of these bacteria
92 (16–18), yielding a range of bacterial phyla, such as Acidobacteria, Bacteroidetes, and
93 Verrucomicrobia, as potential producers of brGDGTs in the environment (16–18).
94 Among these microbes, Acidobacteria were suspected to be the most likely biological
95 sources of brGDGTs (12), because particularly high abundances of brGDGTs
96 correspond with the dominance of Acidobacteria in the bacterial community in soils
97 and peats (18). This was finally confirmed by the examination of the lipid profiles of
98 more than 40 Acidobacterial strains, revealing their widespread production of the
99 potential building block (*iso*-diabolic acid) for brGDGTs, and, most importantly, the
100 positive identification of brGDGT-Ia, a tetramethylated brGDGT, in *Edaphobacter*
101 *aggregans* Wbg-1 and *Acidobacteriaceae* bacteria A2-4c (12, 19, 20). Subsequent work
102 has shown that oxygen limitation can trigger the production of more brGDGT-Ia in *E.*
103 *aggregans* (13), likely explaining the long-observed association of brGDGTs with low
104 oxygen conditions. However, the majority of brGDGTs that are used in climate proxies
105 were absent from the lipid profiles of Acidobacteria previously examined in cultures
106 (12, 19, 20). This necessitates a further search for the biological source(s) of brGDGTs
107 in the environment.

Recently, tetraether synthase (Tes), a key protein responsible for the formation of archaeal isoprenoid GDGTs (isoGDGTs) via the combination of two archaeol molecules, has been identified (21). Bacterial brGDGTs bear a structural resemblance to archaeal isoGDGTs, i.e., both of them consisting of two alkyl chains linked to two glycerol backbones via four ether bonds (15). The Tes protein could, therefore, also be involved in the biosynthesis of bacterial brGDGTs, since Tes homologs have been found in bacterial genomes of diverse phyla including Acidobacteria (21).

In this study, we identified a brGDGT-producing strain *Candidatus Solibacter usitatus* Ellin6076, a member of Acidobacteria subdivision 3, through searching archaeal Tes homologs in bacterial genomes. Crucially, strain Ellin6076 can synthesize regular brGDGTs with more than 4 methyl groups and cyclopentane moieties as its major membrane lipids. This allows us to assess the physiological basis for the brGDGT responses to changes in temperature, pH, and oxygen level, which provides insights into the underlying mechanism of brGDGT-based paleoclimate proxies.

Results

Identification of brGDGTs in Acidobacteria culture. Following our hypothesis that the Tes homolog protein is associated with bacterial brGDGT production, we searched for Tes homologs in bacterial genomes to determine the potential biological source of brGDGTs. Strain Ellin6076 was noteworthy, as it has one Tes homolog with high sequence alignment scores (identity = 40%, e-value = $1e^{-139}$) with archaeal functional

Tes (MA_1486). Moreover, it also contains a possible archaeal GDGT ring synthase (Grs) (22) homolog (identity = 25%, e-value = $1e^{-40}$). We cultured strain Ellin6076 aerobically under optimal growth conditions at 25 °C and pH 5.5 for 14 days, and then identified its lipid profile with reversed-phase–liquid chromatography–high-resolution mass spectrometer (RP–LC–HRMS) and normal-phase–liquid chromatography–mass spectrometer (NP–LC–MS). The results showed that strain Ellin6076 produced a series of brGDGT compounds, including brGDGT-Ia, Ib, Ic, IIa, IIb, IIc, and IIIa. The brGDGT-IIIb and IIIc components were not detected, perhaps due to their absence or concentrations below the detection limit. Compounds anticipated to be related to brGDGT biosyntheses, such as *iso*C_{15}-dialkyl glycerol ether (DGE), branched glycerol trialkyl glycerol tetraethers (brGTGTs), and branched glycerol dialkanol diethers (brGDDs), were also detected. The intact polar lipids (IPLs) corresponding to some of the above core lipids were also identified (Fig. 1; *SI Appendix*, Fig. S1–3).

The harvested cell mass was treated with acid hydrolysis to increase the yield of core lipids for the analyses of brGDGTs and their core lipid derivatives. The fragmentation patterns of five representative compounds are shown as examples in Fig. 1A. The MS^2 behavior of *iso*C_{15}-DGE corresponds to the loss of one *iso*C_{15}-alkyl chain, resulting in a product ion of *m/z* 303.28 ($[C_{18}H_{38}O_3+H]^+$). This characteristic fragment ion is also present in the MS^2 spectra of brGTGT-Ia as reported by Halamka et al. (2021) (13). The MS^2 spectrum of brGDGT-Ia exhibits a featured product ion of *m/z* 603.56 ($[C_{36}H_{74}O_6+H]^+$) and brGDGT-IIb exhibits an additional product ion of *m/z*

615.55 ($[C_{37}H_{74}O_6+H]^+$), both of which are regular fragments observed in the MS^2 spectra of brGDGT compounds (23).

To further determine the alkyl chain structures of brGDGT-IIIa isomers, brGDGT-IIIa purified from the total lipid extract of the hydrolyzed cells cultured at 10 °C was subjected to ether cleavage. The released alkanes were analyzed by gas chromatography–mass spectrometer (GC–MS). Three alkanes, including 13,16-dimethyloctacosane (m2), 5,13,16-trimethyloctacosane (m3), and 5,13,16,24-tetramethyloctacosane (m4), were found, indicating that brGDGT-IIIa was composed of two co-eluting isomers, i.e., one consisting of m2 and m4, and the other consisting of two m3 (Fig. 1B). The alkyl chain structures of the two brGDGT-IIIa isomers can also be confirmed by the fragment ions of *m/z* 631.59 ($[C_{38}H_{78}O_6+H]^+$) and *m/z* 617.57 ($[C_{37}H_{76}O_6+H]^+$) in the mass spectra of IIIa, which correspond to a neutral loss of m2 and m3 in $IIIa_{(m2+m4)}$ and $IIIa_{(m3+m3)}$, respectively (Fig. 1A). The estimated ratio of 82%:18% between $\%IIIa_{(m3+m3)}$ and $\%IIIa_{(m2+m4)}$ (the abundance percentage of IIIa isomers in total IIIa) suggests more $IIIa_{(m3+m3)}$ was produced in the culture of strain Ellin6076, consistent with the observation in a peat sample (24).

The brGDGTs found in the environment contain isomers with an outer methyl group at either the α/ω5 or α/ω6 position, i.e. C_5-methylated and C_6-methylated brGDGTs (2). To determine which brGDGT isomers are produced by strain Ellin6076, we used a soil sample containing both C_5- and C_6-methylated brGDGTs as a reference, and compared the chromatogram and the retention time of target compounds using NP–

LC–MS. The results showed that strain Ellin6076 produced C_5-methylated brGDGTs (*SI Appendix*, Fig. S4). This is also confirmed by the GC–MS analysis of alkyl chains released from the ether cleavage of purified brGDGT-IIIa (Fig. 1B) and brGDGT-IIa (*SI Appendix*, Fig. S5).

To analyze the head groups of brGDGTs, we extracted IPLs from harvested cell mass with a modified Bligh-Dyer method. Phosphohexose (PH) was the most common polar head group detected in the culture, and this has also been identified in peat samples (25). IPLs such as PH-*iso*C_{15}-DGE, PH-brGDGT-Ia, and PH-brGDGT-Ia-PH were identified and confirmed by MS^2 spectra (*SI Appendix* Fig. S3).

The abundance of brGDGTs in Acidobacteria cells. To estimate the proportion of brGDGTs in the total lipids of strain Ellin6076, the core lipid inventory of Ellin6076 cells was analyzed by gas chromatography–mass spectrometer (GC–MS) and NP–LC–MS. Strain Ellin6076 contains a variety of lipids including fatty acids, brGDGTs, hopanoids, and 3-hydroxy fatty acids. The total abundance of regular fatty acids, including saturated and unsaturated $C_{15–20}$ fatty acids, was 13.8 fg/cell, accounting for 30% of the total quantified lipids. On the other hand, the abundance of all brGDGTs, including brGTGTs, was 30.3 fg/cell, accounting for 66% of the total lipids (Fig. 2). Compared to fatty acids and brGDGTs, *iso*C_{15} glycerol ethers including *iso*C_{15}-monoalkyl glycerol ether (MGE) and *iso*C_{15}-DGE had a much lower abundance, 0.9–1.8 fg/cell. Other lipids such as 3-hydroxy fatty acids and hopanoids were minor, with

193 the summed abundance < 0.5 fg/cell (*SI Appendix,* Table S1). Intriguingly, *iso*-diabolic
194 acids were absent from the lipid profile of strain Ellin6076. The fractional abundance
195 of brGDGTs in the total lipids of strain Ellin6076 is much higher than that in *E.*
196 *aggregans*, whose brGDGTs account for only approximately 3% of total lipids (13).
197 Our findings demonstrate that some Acidobacteria, such as Ellin6076, use the
198 membrane-spanning lipids brGDGTs and fatty acids as major components to form
199 unique cell membranes with a mixed monolayer and bilayer structure (Fig. 2C).
200
201 **The response of brGDGTs to cultivation conditions in Acidobacteria culture.** The
202 production of multiple brGDGTs by the strain Ellin6076 allows us to directly assess the
203 brGDGT changes under controlled experimental conditions. We cultured strain
204 Ellin6076 independently at temperatures ranging from 10–35 °C and pH ranging from
205 4.5–6.5 (*SI Appendix,* Fig. S6). Then we evaluated the changes in the fractional
206 abundance of brGDGT-Ia, Ib, IIa, IIb, and IIIa, since these components are critical for
207 the calculation of brGDGT-based proxies (e.g. MBT'$_{5ME}$ and CBT$_{5ME}$).
208 The MBT'$_{5ME}$ index, expressing the methylation degree of C_5-methylated
209 brGDGTs showed a significant positive correlation with culture temperature (10 °C to
210 25 °C), having a determination coefficient (R^2) up to 0.97 (Fig. 3A). Specifically, %Ia,
211 the abundance percentage of brGDGT-Ia in total brGDGTs, increased with temperature
212 in this range, while %IIa and %IIIa decreased (*SI Appendix,* Fig. S7, and Table S2).
213 Importantly, the MBT'$_{5ME}$ values at 30 °C and 35 °C were nearly 1.00 (*SI Appendix*,

Table S2), the upper limit of this index. BrGDGT-Ia was overwhelmingly dominant at 30 °C (%Ia > 93%) and 35 °C (%Ia > 97%), consistent with environmental studies and confirming that the MBT'$_{5ME}$ index is insensitive to temperature changes above 25 °C. Excluding these data showed a remarkable influence of temperature on the distributions of C_5-methylated brGDGTs and the MBT'$_{5ME}$ index in the culture of strain Ellin6076.

The cyclization degree of brGDGTs was assessed by the CBT index, with a higher CBT value indicating a lower degree of cyclization (7). A positive correlation between CBT$_{5ME}$ and pH from pH 4.5 to 6.5 was found for the culture samples, opposed to the general negative relationship derived from the global soil database (2, 7) (Fig. 3B).

In addition to temperature and pH, we also examined whether strain Ellin6076 adjusts its brGDGT composition in response to oxygen limitation. When strain Ellin6076 was cultured under oxygen limitation (1% O_2 concentration, 25 °C, pH 5.5), the abundance of total brGDGTs decreased to 10 fg/cell compared to 30 fg/cell under aerobic condition (21% O_2 concentration, 25 °C, pH 5.5), in contrast to the enhanced production under low oxygen reported in *E. aggregans* (13). Intriguingly, %IIa and %IIIa increased and %Ib, %Ic, and %IIb decreased under the stress of low oxygen. %Ia was effectively constant (87–91%) under both conditions (*SI Appendix*, Fig. S9 and Table S2). Consequently, MBT'$_{5ME}$ values slightly decreased but CBT$_{5ME}$ values strikingly increased under oxygen limitation (Fig. 3C).

Discussion

The conundrum of brGDGT-producers. The biological sources of brGDGTs in the environment have puzzled many scientists for more than two decades. Despite substantial effort devoted to solving this conundrum (12, 13, 16, 18–20, 26–28), a bacterial pure culture producing the multiple brGDGTs that have been used to construct paleoclimate has been lacking. Here, we found a bacterial strain Ellin6076 is capable of synthesizing multiple brGDGTs as its major cell membrane lipids. This is a crucial step towards understanding the source of diverse brGDGTs in the environment via culturing under different conditions, shedding new insights into the ecophysiology and taxonomy of brGDGT-producers.

Several lines of evidence, in particular from peats, suggest that brGDGT-producers might be anaerobic or facultative anaerobic bacteria (15, 18, 27). However, strain Ellin6076 is an obligately aerobic bacteria, indicating that at least a portion of brGDGTs in peats, soils, and lakes can be produced by aerobic Acidobacteria. This is consistent with one order of magnitude higher rates of brGDGT production in incubations with surface peat under oxic conditions than anoxic deeper peats (27), as well as the occurrence of abundant *in situ* brGDGTs produced in oxic lake water columns (29). However, these observations are inconsistent with the increased production of brGDGTs by *E. aggregans* under low O_2 concentrations (13) and the high abundance of brGDGTs in low oxygen environments (15, 18). It is likely that brGDGTs are synthesized by a range of bacteria and/or at least some observations from the

environment reflect preservation of brGDGTs in anoxic settings rather than higher production. Strain Ellin6076 uses glucose as the carbon source for the chemoheterotrophic lifestyle, consistent with the previous views on the lifestyle of brGDGT-producers based on the carbon isotopic compositions of brGDGTs in the environment (27, 30).

The previous identification of brGDGT-Ia in two Acidobacteria belonging to subdivision 1, together with the occurrence of more diverse brGDGTs in Ellin6076, indicates different Acidobacteria can produce completely distinct brGDGT profiles. This suggests that at least some variations in environmental brGDGT distributions reflect community change rather than physiological adaptations within a single taxon. In altitudinal or latitudinal transects with a large temperature or pH gradient, the impact of these environmental factors on brGDGTs overwhelmingly exceeds the community effect, resulting in significant correlations between brGDGT distribution and temperature or pH (9, 31, 32); however, at local scales, the community effect can dominate, as De Jonge et al. previously observed in high and mid-latitude soils (33, 34). It is, therefore, necessary to evaluate the community effect on existing brGDGT paleoclimate proxies in their applications to paleo-reconstructions.

For example, the occurrence of tetramethylated brGDGTs and C_5-methylated brGDGTs with an absence of C_6-methylated brGDGTs in Ellin6076 suggests that C_5- and C_6-methylated brGDGTs are produced by different (Acido)bacteria. The relative abundance of C_6- vs. C_5-methylated brGDGTs (generally expressed in the IR_{6ME} proxy)

277 appears to be dependent on pH or salinity in a variety of environmental samples (10,
278 35, 36). This study suggests that pH proxies based upon the relative abundance of C_6-
279 vs. C_5-methylated brGDGTs are essentially regulated by a shift in the Acidobacteria
280 community. Ellin6076 falls within Acidobacteria subdivision 3, a clade that is abundant
281 in acidic soils and peats (37–39), agreeing well with the dominance of C_5-methylated
282 brGDGTs over their C_6-methylated isomers in these environments (9, 10). Future work
283 should ascertain the biological source(s) of C_6-methylated brGDGTs, perhaps by
284 examining Acidobacteria with a Tes homolog that are abundant in alkaline
285 environments, e.g. Acidobacteria subdivision 4 and 6.
286
287 **The physiological function of methylation and cyclization in brGDGTs.** Our strain
288 Ellin6076 culture experiments allow direct examination of how methylation and
289 cyclization of brGDGTs in a single species respond to different temperature, pH and
290 oxygen conditions. Canonically, modifications in the degree of methylation and
291 cyclization are thought to be a microbial strategy – homeoviscous or homeostatic
292 adaptation – to adapt to ambient environmental change (40, 41). Microbes modulate
293 their lipid compositions to maintain appropriate fluidity and permeability of cell
294 membranes (42, 43). Bacteria can modify the degree of branching in their fatty acids at
295 varying temperatures (44), for example, with more branched-chain fatty acids observed
296 at 45 °C than at 65 °C in the culture of a thermophilic bacteria *Bacillus*
297 *stearothermophilus* (45). We observed a similar modification in Ellin6076, which

298 produced more C_5-methylated brGDGTs (e.g. brGDGT-IIa and IIIa) and fewer
299 tetramethylated brGDGT-Ia, thereby increasing the degree of methylation, at
300 temperatures below 25 °C. Recent molecular dynamics simulations of bacterial
301 membranes consisting of brGDGTs confirm that a higher degree of methylation results
302 in a less rigid and more fluid membrane (46). Our culturing experiments support this
303 theory and suggest that the increase in brGDGT methylation is a physiological
304 adaptation strategy for brGDGT-producing bacteria in cold conditions. In contrast, pH
305 and oxygen limitation exert a minor effect on the degree of brGDGT methylation (*SI*
306 *Appendix*, Fig. S8 and Fig. S9).

307 The degree of cyclization in isoGDGTs is a key strategy for archaea to adapt to
308 extreme environments, with more cyclopentyl moieties generally produced by archaea
309 growing at a higher temperature or a lower pH (47–49). Molecular modeling suggests
310 that an increase in isoGDGT cyclization degree leads to tighter membrane packing that
311 enhances membrane thermal stability and reduces overall membrane permeability (50,
312 51). Given the similarity in structure, it is reasonable to hypothesize that cyclopentane
313 rings in brGDGTs have a similar function. Indeed, our results demonstrate that lower
314 pH and higher temperature generally cause a higher degree of brGDGT cyclization (*SI*
315 *Appendix*, Fig. S7 and Fig. S8), which is consistent with the behaviour of isoGDGTs in
316 a thermoacidophilic archaeon *Sulfolobus acidocaldarius* (49). However, this
317 relationship is opposite to the well-established empirical relationship of soil pH with
318 the degree of brGDGT cyclization. This could mean that Ellin6076 (or our culture

conditions) are atypical or that brGDGT cyclization is sensitive to multiple variables, instead of pH alone. Given the similarity in behaviour between the cyclization of Ellin6076 brGDGTs and that in archaea, as well as the predictions of molecular modelling, we instead propose that the widely observed environmental relationship documents changes in the brGDGT-producing community rather than an ecophysiological relationship.

Implications for brGDGT-based temperature and pH proxies. The physiological function of methylation and cyclization in brGDGTs helps to interpret MBT and CBT proxies and their relationships with environmental factors in nature. The positive correlation between MBT'$_{5ME}$ and temperature for the culture of Ellin6076 is consistent with the empirical observation of global soils (Fig. 3A). The calibration equation for the strain Ellin6076 is:

$$\text{MBT'}_{5ME} = 0.047 \times T - 0.22 \ (R^2 = 0.97, p < 0.0001, n = 12) \qquad [1]$$

The slope of the regression line for strain Ellin6076 is significantly steeper than that for the global soil dataset. There could be two explanations for this. First, the majority of brGDGTs in soils are produced by other (Acido)bacteria species with a brGDGT response to temperatures differing from the strain Ellin6076. Second, the MBT'$_{5ME}$ for global soils could record the growing season temperatures. The difference in MBT'$_{5ME}$ values between the strain Ellin6076 and global soils increases with decreasing temperature, which might relate to the increased seasonal production of

340 brGDGTs in colder soils. The strain Ellin6076 cannot grow well below 10 °C. Likewise,
341 Acidobacteria producing brGDGTs in soils are unlikely to proliferate at a low
342 temperature. If the MBT'$_{5ME}$-temperature calibration for the strain Ellin6076 is applied
343 to the global soils, the temperature estimates for soils from cold regions would be
344 significantly higher than the mean annual air temperature (MAT). In contrast, the
345 MBT'$_{5ME}$ values for the strain Ellin6076 agree well with those for global soils at
346 temperatures > 20 °C, where the effect of temperature seasonality is minor. This
347 suggests caution in the application of brGDGT temperature proxies in low temperature
348 contexts. At the same time, MBT'$_{5ME}$ values reached saturation at 25 °C in the culture
349 experiments (*SI Appendix*, Table S2), which is consistent with the observations in soils,
350 suggesting the MBT'$_{5ME}$ index cannot be used to reconstruct temperature changes
351 above that (Fig. 3A).

352 Temperature was the only factor controlling MBT'$_{5ME}$ variation in the culture
353 experiment, whereas other environmental variables such as pH and oxygen availability
354 exerted only minor effects on this index. The MBT'$_{5ME}$ values for strain Ellin6076
355 barely changed under different pH conditions (*SI Appendix*, Table S2) and decreased
356 only slightly under oxygen limitation (Fig. 3C). This suggests that pH and oxygen
357 availability could be excluded as potential factors affecting the MBT'$_{5ME}$ in the
358 environment. However, this only applies at the species level. Several previous studies
359 showed that soil pH or oxygen level are key factors that determine the variation of
360 MBT'$_{5ME}$ in soils and peats (10, 52, 53). We attribute this to the community effect

361 inferred above. A shift in the Acidobacteria community would cause a change in
362 brGDGT distribution since some Acidobacteria can only produce brGDGT-Ia (12, 13),
363 whereas other Acidobacteria like Ellin6076 are capable of synthesizing more diverse
364 brGDGTs. It also appears that changes in pH drive shifts in the Acidobacteria
365 community as documented by the unexpected change in brGDGT cyclization (see
366 above). This could explain why changes in brGDGT-reconstructed pH are sometimes
367 associated with unexpected changes in MBT-derived temperatures (54, 55).

368 In addition, oxygen limitation could trigger the production of more brGDGTs,
369 especially brGDGT-Ia (12, 13). Although not observed in strain Ellin6076, this effect
370 would also increase the MBT'$_{5ME}$ values in soils. While our study demonstrates the
371 robustness of MBT'$_{5ME}$ as a paleothermometer, factors that potentially affect the
372 Acidobacteria community (not limited to oxygen limitation and pH) need to be
373 considered as well.

374 Our work provides fundamental new insights into brGDGT biosynthesis and
375 adaptation. By identifying archaeal tetraether synthase homologs in bacterial genomes,
376 we were able to identify a brGDGT-producing Acidobacterium, strain Ellin6076.
377 Crucially, because this organism shows to produce a suite of brGDGTs, we were able
378 to conduct culture experiments to determine the response of brGDGT distributions to
379 changes in temperature, pH and oxygen. Such work reaffirms confidence in brGDGT-
380 temperature proxies but also suggests that much of the environmental variation in
381 brGDGT distributions ascribed to pH is instead due to community change.

Methods

Strain and Culturing. *Candidatus Solibacter usitatus* Ellin6076 (DSM 22595) was purchased from the German Collection of Microorganisms and Cell Cultures (DSMZ). The strain was routinely cultured in the modified liquid MM medium under the optimal growth conditions aerobically at 25 °C and pH 5.5 for 14 days to reach the stationary phase. To investigate how brGDGT distribution responds to environmental changes, strain Ellin6076 was cultured under different temperatures (10–35 °C), pH values (4.5–6.5), and oxygen levels (1% vs. 21% O_2 concentration in the headspace). All the experiments were performed in biological triplicates. The details of culturing experiments are described in *SI Appendix*.

Lipid Extraction and Analyses. Culture samples were harvested at the stationary phase and collected by 10,000 × g centrifugation for 15 min and cell pellets were kept at –80 °C before further experiments. An aliquot of wet cell mass was treated with acid hydrolysis for core lipid (CL) analysis, and another aliquot was directly extracted using a modified Bligh-Dyer method for intact polar lipid (IPL) analysis as described in *SI Appendix*.

BrGDGTs together with their CL and IPL derivatives were identified using a Waters ACQUITY I-Class Ultra-performance liquid chromatography (UPLC) coupled to SYNAPT G2-S*i* quadrupole time-of-flight (qTOF) high-resolution mass spectrometer. The quantification of brGDGTs with the C_{46} GTGT internal standard was performed on an Agilent 1260 series high-performance liquid chromatography (HPLC)

system coupled with Agilent 6135B quadrupole mass spectrometer. The CL inventory including fatty acids, mono/dialkyl glycerol ethers, and other lipids in the cultures was analyzed by a Thermo Finnigan Trace 1300 gas chromatography coupled to an ISQ 7000 mass spectrometer (GC–MS). The purification and ether cleavage were performed on target compounds such as brGDGT-IIa and IIIa to further determine the methyl positions of brGDGTs and co-eluting isomers of IIIa produced by strain Ellin6076. The alkanes released from brGDGTs were analyzed by GC and GC–MS. The details of lipid extraction, analyses, identification and quantification are described in *SI Appendix*.

Calculation of MBT and CBT proxies. We used MBT'_{5ME} and CBT_{5ME} proxies following De Jonge et al. (2014) to evaluate the distribution of brGDGTs (2), as only C_5-methyl isomers were identified in strain Ellin6076. The calculation was based on the relative abundances of major brGDGTs:

$$MBT'_{5ME} = \frac{Ia + Ib + Ic}{Ia + Ib + Ic + IIa + IIb + IIc + IIIa} \quad [2]$$

$$CBT_{5ME} = -\log_{10}\left(\frac{Ib+IIb}{Ia+IIa}\right) \quad [3]$$

Acknowledgments

We thank Wenyong Yao, Wan Zhang, and Jing Guo for microscopy observation and cell counting. This study was supported by the National Natural Science Foundation of China (No. 92051112 to Z.Z., No. 32170041 to Z.Z., and No. 42073072 to H.Y.), the Science, Technology, and Innovation Commission of Shenzhen Municipality (No. 20200925154325002 to Z.Z.), the Southern Marine Science and Engineering Guangdong Laboratory (Guangzhou) (No. K19313901), and the Shenzhen Key Laboratory of Marine Archaea Geo-Omics, Southern University of Science and Technology (No. ZDSYS201802081843490).

Figure Legends

Fig. 1. Identification of brGDGTs in strain Ellin6076 by RP–LC–HRMS and GC–MS. *(A)* Extracted ion chromatograms (EIC) and MS^2 mass spectra of five representative compounds analyzed by RP–LC–HRMS are shown. *(B)* The partial total ion chromatogram (TIC) and mass spectra of brGDGT-IIIa derived alkyl chains analyzed by GC–MS are shown. $IIIa_{(m2+m4)}$ and $IIIa_{(m3+m3)}$ represent co-eluting isomers of brGDGT-IIIa with distinct alkyl chains. The m2, m3, and m4 refer to the alkyl chains with 2, 3, and 4 methyl groups, respectively. The precursor ions, such as $[M+H]^+$ in RP–LC–HRMS and $[M^+–15]$ in GC–MS, are marked with stars. The characteristic product ions are marked by colors and fragment positions are denoted by dash lines. The pie chart shows the proportion of IIIa isomers in total IIIa. The calculation is based on the results of GC analysis and the contribution of co-eluting IIa to m2 and m3 in Fig. 1B is subtracted as described in *SI Appendix*.

Fig. 2. The lipid profile of strain Ellin6076. *(A)* The cellular contents and *(B)* the fractional abundances of major lipids in strain Ellin6076. The cellular content of brGDGTs includes that of brGTGTs, and the cellular content of *iso*C_{15} glycerol ethers includes that of *iso*C_{15}-MGE and *iso*C_{15}-DGE (*SI Appendix*, Table S1). Error bars represent the standard deviations among mean values of biological triplicate. The quantification is based on internal standards and cell amounts as described in *SI Appendix*. (*C*) Schematic cell membrane of strain Ellin6076 containing monolayer and bilayer structures with proposed permeability trend.

Fig. 3. Relationships between brGDGT-based proxies and environmental factors. *(A)* The MBT'_{5ME} vs. temperature in the culture of strain Ellin6076 (red line) together with the MBT'_{5ME} in the global soil database (gray line; De Jonge et al., 2014). The data at 30 °C and 35 °C are excluded from the linear regression. *(B)* The CBT_{5ME} vs. pH in the culture of strain Ellin6076 (blue line) and the global soil database (gray line; De Jonge et al., 2014). The shaded area and dash lines show 95% confidence interval and 95% prediction interval of the linear regression, respectively. *(C)* The comparison of MBT'_{5ME} and CBT_{5ME} values between oxygen limitation and aerobic condition. Each biological replicate is displayed and lines represent the mean values.

References

1. R. E. Summons, P. V Welander, D. A. Gold, Lipid biomarkers: molecular tools for illuminating the history of microbial life. *Nat. Rev. Microbiol.* **20**, 174–185 (2022).
2. C. De Jonge, *et al.*, Occurrence and abundance of 6-methyl branched glycerol dialkyl glycerol tetraethers in soils: Implications for palaeoclimate reconstruction. *Geochim. Cosmochim. Acta* **141**, 97–112 (2014).
3. S. Schouten, E. C. Hopmans, J. S. Sinninghe Damsté, The organic geochemistry of glycerol dialkyl glycerol tetraether lipids: A review. *Org. Geochem.* **54**, 19–61 (2013).
4. E. C. Hopmans, *et al.*, A novel proxy for terrestrial organic matter in sediments based on branched and isoprenoid tetraether lipids. *Earth Planet. Sci. Lett.* **224**, 107–116 (2004).
5. H. Wang, W. Liu, C. L. Zhang, Dependence of the cyclization of branched tetraethers on soil moisture in alkaline soils from arid-subhumid China: Implications for palaeorainfall reconstructions on the Chinese Loess Plateau. *Biogeosciences* **11**, 6755–6768 (2014).
6. G. N. Inglis, *et al.*, Biomarker approaches for reconstructing terrestrial environmental change. *Annu. Rev. Earth Planet. Sci.* **50**, 369–394 (2022).
7. J. W. H. Weijers, S. Schouten, J. C. van den Donker, E. C. Hopmans, J. S. Sinninghe Damsté, Environmental controls on bacterial tetraether membrane lipid distribution in soils. *Geochim. Cosmochim. Acta* **71**, 703–713 (2007).
8. F. Peterse, *et al.*, Revised calibration of the MBT–CBT paleotemperature proxy based on branched tetraether membrane lipids in surface soils. *Geochim. Cosmochim. Acta* **96**, 215–229 (2012).
9. B. D. A. Naafs, A. V. Gallego-Sala, G. N. Inglis, R. D. Pancost, Refining the global branched glycerol dialkyl glycerol tetraether (brGDGT) soil temperature calibration. *Org. Geochem.* **106**, 48–56 (2017).
10. B. D. A. Naafs, *et al.*, Introducing global peat-specific temperature and pH calibrations based on brGDGT bacterial lipids. *Geochim. Cosmochim. Acta* **208**, 285–301 (2017).
11. P. Martínez-Sosa, *et al.*, A global Bayesian temperature calibration for lacustrine brGDGTs. *Geochim. Cosmochim. Acta* **305**, 87–105 (2021).
12. J. S. Sinninghe Damsté, *et al.*, 13,16-Dimethyl octacosanedioic acid (*iso*-Diabolic Acid), a common membrane-spanning lipid of *Acidobacteria* subdivisions 1 and 3. *Appl. Environ. Microbiol.* **77**, 4147–4154 (2011).
13. T. A. Halamka, *et al.*, Oxygen limitation can trigger the production of branched GDGTs in culture. *Geochemical Perspect. Lett.* **19**, 36–39 (2021).
14. J. S. Sinninghe Damsté, E. C. Hopmans, R. D. Pancost, S. Schouten, J. A. J. Geenevasen, Newly discovered non-isoprenoid glycerol dialkyl glycerol tetraether lipids in sediments. *Chem. Commun.* **17**, 1683–1684 (2000).

15. J. W. H. Weijers, *et al.*, Membrane lipids of mesophilic anaerobic bacteria thriving in peats have typical archaeal traits. *Environ. Microbiol.* **8**, 648–657 (2006).
16. C. L. Zhang, *et al.*, In situ production of branched glycerol dialkyl glycerol tetraethers in a great basin hot spring (USA). *Front. Microbiol.* **4**, 181 (2013).
17. J. Guo, *et al.*, Soil pH and aridity influence distributions of branched tetraether lipids in grassland soils along an aridity transect. *Org. Geochem.* **164**, 104347 (2021).
18. J. W. H. Weijers, *et al.*, Constraints on the biological source(s) of the orphan branched tetraether membrane lipids. *Geomicrobiol. J.* **26**, 402–414 (2009).
19. J. S. Sinninghe Damsté, *et al.*, Ether- and ester-bound *iso*-diabolic acid and other lipids in members of *Acidobacteria* subdivision 4. *Appl. Environ. Microbiol.* **80**, 5207–5218 (2014).
20. J. S. Sinninghe Damsté, *et al.*, An overview of the occurrence of ether- and ester-linked *iso*-diabolic acid membrane lipids in microbial cultures of the Acidobacteria: Implications for brGDGT paleoproxies for temperature and pH. *Org. Geochem.* **124**, 63–76 (2018).
21. Z. Zeng, *et al.*, Identification of a protein responsible for the synthesis of archaeal membrane-spanning GDGT lipids. *Nat. Commun.* **13**, 1545 (2022).
22. Z. Zeng, *et al.*, GDGT cyclization proteins identify the dominant archaeal sources of tetraether lipids in the ocean. *Proc. Natl. Acad. Sci. U. S. A.* **116**, 22505–22511 (2019).
23. X.-L. Liu, R. E. Summons, K.-U. Hinrichs, Extending the known range of glycerol ether lipids in the environment: structural assignments based on tandem mass spectral fragmentation patterns. *Rapid Commun. Mass Spectrom.* **26**, 2295–2302 (2012).
24. C. De Jonge, *et al.*, Identification of novel penta- and hexamethylated branched glycerol dialkyl glycerol tetraethers in peat using HPLC–MS^2, GC–MS and GC–SMB-MS. *Org. Geochem.* **54**, 78–82 (2013).
25. F. Peterse, *et al.*, Identification and distribution of intact polar branched tetraether lipids in peat and soil. *Org. Geochem.* **42**, 1007–1015 (2011).
26. Y. Chen, *et al.*, Branched GDGT production at elevated temperatures in anaerobic soil microcosm incubations. *Org. Geochem.* **117**, 12–21 (2018).
27. A. Huguet, *et al.*, Production rates of bacterial tetraether lipids and fatty acids in peatland under varying oxygen concentrations. *Geochim. Cosmochim. Acta* **203**, 103–116 (2017).
28. P. Martínez-Sosa, J. E. Tierney, Lacustrine brGDGT response to microcosm and mesocosm incubations. *Org. Geochem.* **127**, 12–22 (2019).
29. J. Wu, *et al.*, Variations in dissolved O_2 in a Chinese lake drive changes in microbial communities and impact sedimentary GDGT distributions. *Chem. Geol.* **579**, 120348 (2021).
30. J. W. H. Weijers, G. L. B. Wiesenberg, R. Bol, E. C. Hopmans, R. D. Pancost,

Carbon isotopic composition of branched tetraether membrane lipids in soils suggest a rapid turnover and a heterotrophic life style of their source organism(s). *Biogeosciences* **7**, 2959–2973 (2010).

31. V. J. Anderson, T. M. Shanahan, J. E. Saylor, B. K. Horton, A. R. Mora, Sources of local and regional variability in the MBT'/CBT paleotemperature proxy: Insights from a modern elevation transect across the Eastern Cordillera of Colombia. *Org. Geochem.* **69**, 42–51 (2014).
32. H. Yang, *et al.*, The 6-methyl branched tetraethers significantly affect the performance of the methylation index (MBT') in soils from an altitudinal transect at Mount Shennongjia. *Org. Geochem.* **82**, 42–53 (2015).
33. C. De Jonge, *et al.*, Lipid biomarker temperature proxy responds to abrupt shift in the bacterial community composition in geothermally heated soils. *Org. Geochem.* **137**, 103897 (2019).
34. C. De Jonge, *et al.*, The influence of soil chemistry on branched tetraether lipids in mid- and high latitude soils: Implications for brGDGT-based paleothermometry. *Geochim. Cosmochim. Acta* **310**, 95–112 (2021).
35. H. Wang, *et al.*, Salinity-controlled isomerization of lacustrine brGDGTs impacts the associated MBT'$_{5ME}$ terrestrial temperature index. *Geochim. Cosmochim. Acta* **305**, 33–48 (2021).
36. H. Wang, Z. An, H. Lu, Z. Zhao, W. Liu, Calibrating bacterial tetraether distributions towards in situ soil temperature and application to a loess-paleosol sequence. *Quat. Sci. Rev.* **231**, 106172 (2020).
37. A. M. Kielak, C. C. Barreto, G. A. Kowalchuk, J. A. van Veen, E. E. Kuramae, The Ecology of *Acidobacteria*: Moving beyond Genes and Genomes. *Front. Microbiol.* **7**, 744 (2016).
38. S. Kalam, *et al.*, Recent Understanding of Soil Acidobacteria and Their Ecological Significance: A Critical Review. *Front. Microbiol.* **11**, 580024 (2020).
39. S. A. Eichorst, *et al.*, Genomic insights into the *Acidobacteria* reveal strategies for their success in terrestrial environments. *Environ. Microbiol.* **20**, 1041–1063 (2018).
40. M. Sinensky, Homeoviscous adaptation: a homeostatic process that regulates the viscosity of membrane lipids in *Escherichia coli*. *Proc. Natl. Acad. Sci. U. S. A.* **71**, 522–525 (1974).
41. J. E. Cronan, E. P. Gelmann, Physical properties of membrane lipids: biological relevance and regulation. *Bacteriol. Rev.* **39**, 232–256 (1975).
42. R. Ernst, C. S. Ejsing, B. Antonny, Homeoviscous Adaptation and the Regulation of Membrane Lipids. *J. Mol. Biol.* **428**, 4776–4791 (2016).
43. Y. M. Zhang, C. O. Rock, Membrane lipid homeostasis in bacteria. *Nat. Rev. Microbiol.* **6**, 222–233 (2008).
44. M. Suutari, S. Laakso, Microbial fatty acids and thermal adaptation. *Crit. Rev. Microbiol.* **20**, 285–328 (1994).

586 45. J. Reizer, N. Grossowicz, Y. Barenholz, The effect of growth temperature on the
587 thermotropic behavior of the membranes of a thermophilic *Bacillus*.
588 Composition-structure-function relationships. *BBA - Biomembr.* **815**, 268–280
589 (1985).
590 46. B. D. A. Naafs, A. S. F. Oliveira, A. J. Mulholland, Molecular dynamics
591 simulations support the hypothesis that the brGDGT paleothermometer is based
592 on homeoviscous adaptation. *Geochim. Cosmochim. Acta* **312**, 44–56 (2021).
593 47. J. Feyhl-Buska, *et al.*, Influence of growth phase, pH, and temperature on the
594 abundance and composition of tetraether lipids in the thermoacidophile
595 *Picrophilus torridus*. *Front. Microbiol.* **7**, 1323 (2016).
596 48. W. Qin, *et al.*, Confounding effects of oxygen and temperature on the TEX_{86}
597 signature of marine Thaumarchaeota. *Proc. Natl. Acad. Sci. U. S. A.* **112**, 10979–
598 10984 (2015).
599 49. A. Cobban, *et al.*, Multiple environmental parameters impact lipid cyclization in
600 *Sulfolobus acidocaldarius*. *Environ. Microbiol.* **22**, 4046–4056 (2020).
601 50. J. L. Gabriel, P. Lee Gau Chong, Molecular modeling of archaebacterial bipolar
602 tetraether lipid membranes. *Chem. Phys. Lipids* **105**, 193–200 (2000).
603 51. A. O. Chugunov, P. E. Volynsky, N. A. Krylov, I. A. Boldyrev, R. G. Efremov,
604 Liquid but durable: Molecular dynamics simulations explain the unique
605 properties of archaeal-like membranes. *Sci. Rep.* **4**, 7462 (2014).
606 52. H. Pei, S. Zhao, H. Yang, S. Xie, Variation of branched tetraethers with soil
607 depth in relation to non-temperature factors: Implications for paleoclimate
608 reconstruction. *Chem. Geol.* **572**, 120211 (2021).
609 53. X. Dang, H. Yang, B. D. A. Naafs, R. D. Pancost, S. Xie, Evidence of moisture
610 control on the methylation of branched glycerol dialkyl glycerol tetraethers in
611 semi-arid and arid soils. *Geochim. Cosmochim. Acta* **189**, 24–36 (2016).
612 54. G. N. Inglis, *et al.*, Terrestrial environmental change across the onset of the
613 PETM and the associated impact on biomarker proxies: A cautionary tale. *Glob.*
614 *Planet. Change* **181**, 102991 (2019).
615 55. J. W. H. Weijers, P. Steinmann, E. C. Hopmans, S. Schouten, J. S. Sinninghe
616 Damsté, Bacterial tetraether membrane lipids in peat and coal: Testing the MBT-
617 CBT temperature proxy for climate reconstruction. *Org. Geochem.* **42**, 477–486
618 (2011).

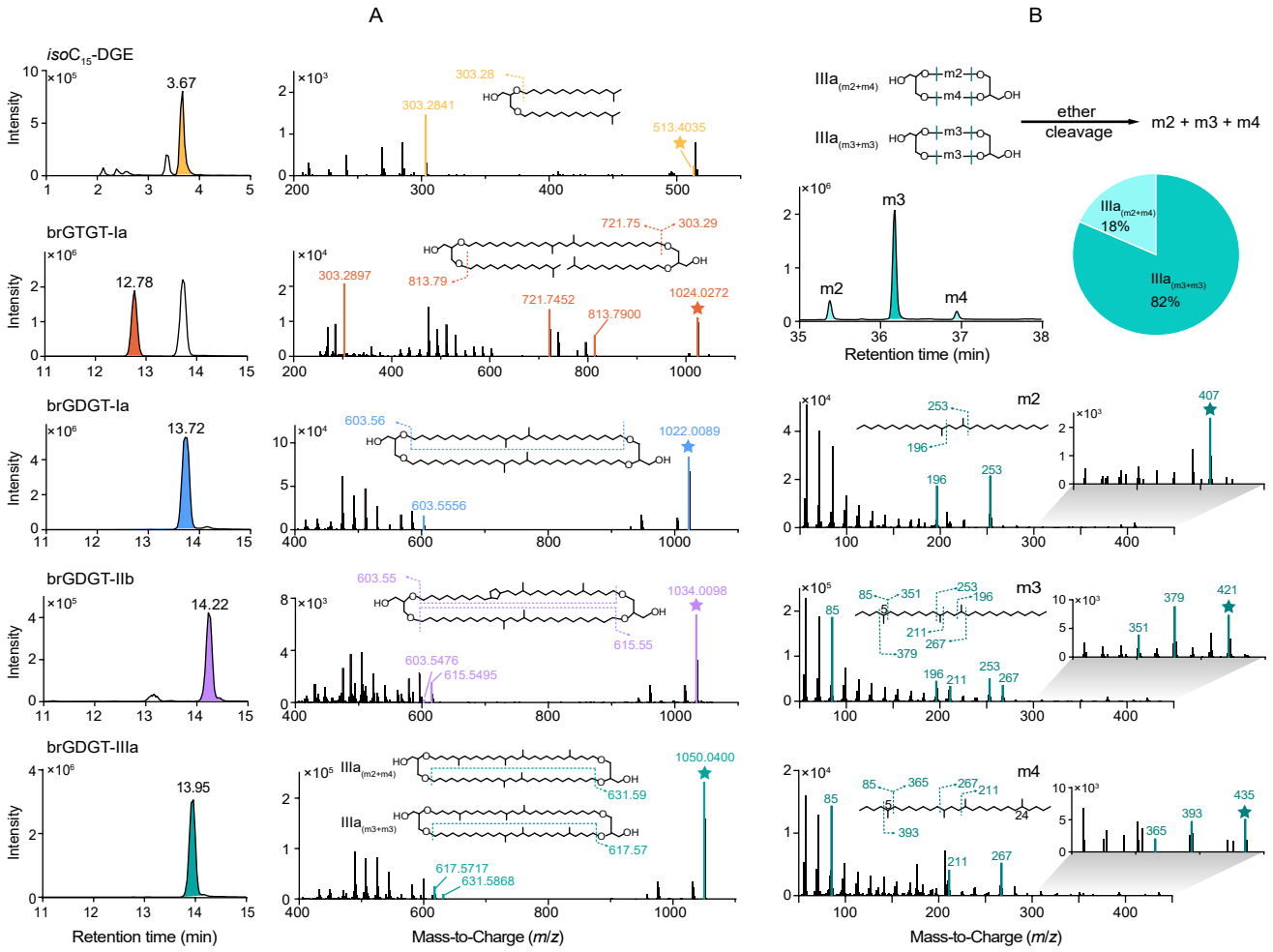

Fig. 1. Identification of brGDGTs in strain Ellin6076 by RP–LC–HRMS and GC–MS. (*A*) Extracted ion chromatograms (EIC) and MS² mass spectra of five representative compounds analyzed by RP–LC–HRMS are shown. (*B*) The partial total ion chromatogram (TIC) and mass spectra of brGDGT-IIIa derived alkyl chains analyzed by GC–MS are shown. $IIIa_{(m2+m4)}$ and $IIIa_{(m3+m3)}$ represent co-eluting isomers of brGDGT-IIIa with distinct alkyl chains. The m2, m3, and m4 refer to the alkyl chains with 2, 3, and 4 methyl groups, respectively. The precursor ions, such as $[M+H]^+$ in RP–LC–HRMS and $[M^+–15]$ in GC–MS, are marked with stars. The characteristic product ions are marked by colors and fragment positions are denoted by dash lines. The pie chart shows the proportion of IIIa isomers in total IIIa. The calculation is based on the results of GC analysis and the contribution of co-eluting IIa to m2 and m3 in Fig. 1B is subtracted as described in *SI Appendix*.

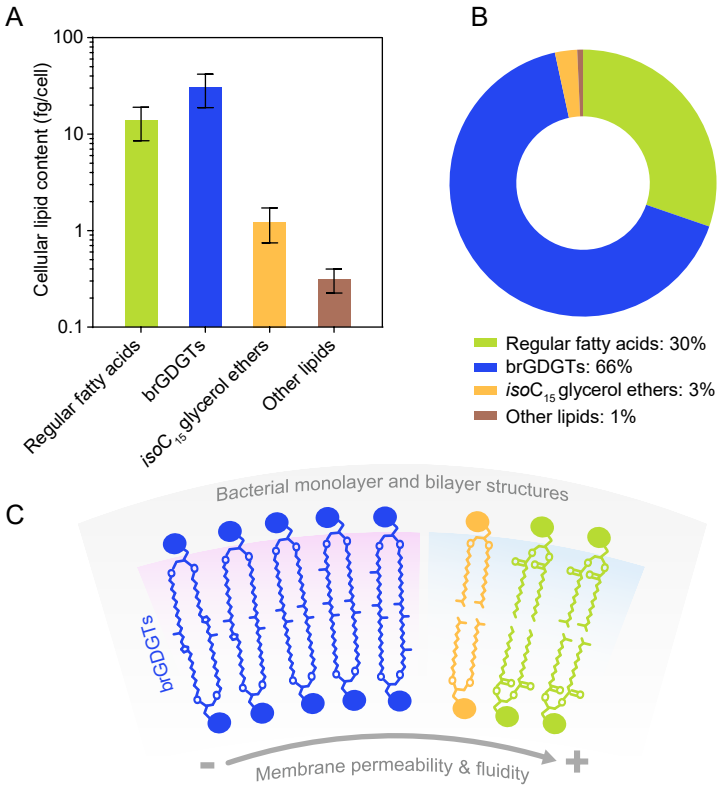

Fig. 2. The lipid profile of strain Ellin6076. (*A*) The cellular contents and (*B*) the fractional abundances of major lipids in strain Ellin6076. The cellular content of brGDGTs includes that of brGTGTs, and the cellular content of isoC$_{15}$ glycerol ethers includes that of isoC$_{15}$-MGE and isoC$_{15}$-DGE (*SI Appendix*, Table S1). Error bars represent the standard deviations among mean values of biological triplicate. The quantification is based on internal standards and cell amounts as described in *SI Appendix*. (*C*) Schematic cell membrane of strain Ellin6076 containing monolayer and bilayer structures with proposed permeability trend.

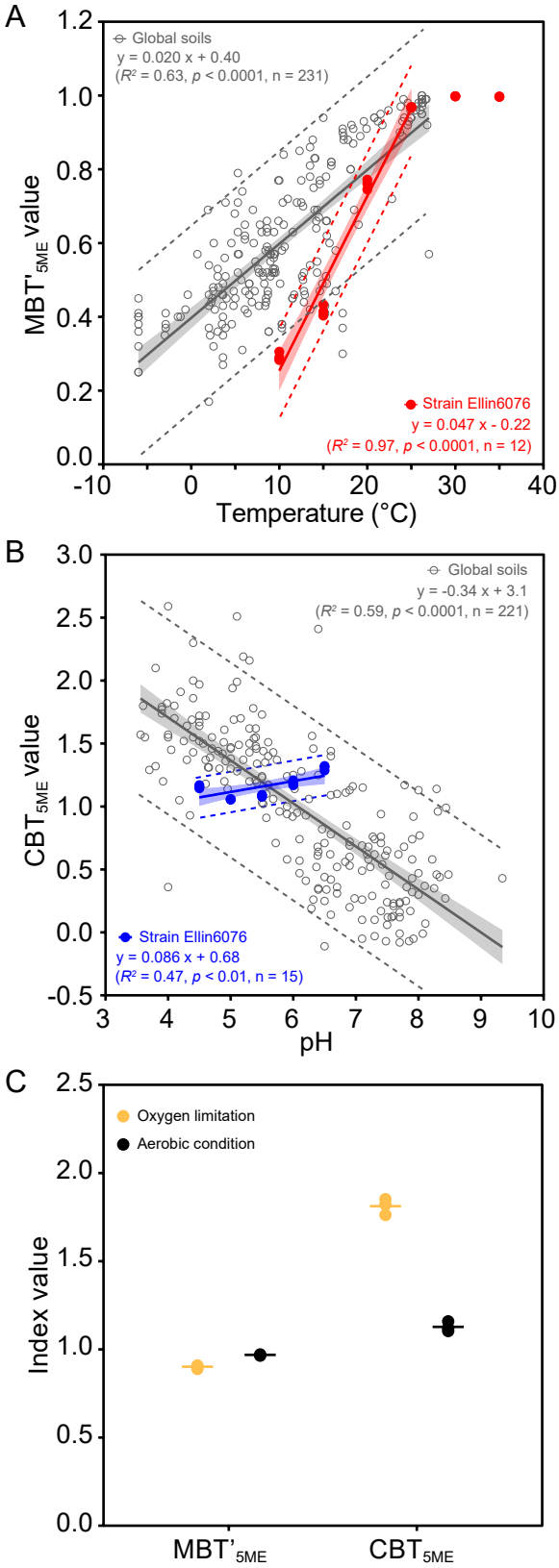

Fig. 3. Relationships between brGDGT-based proxies and environmental factors. (*A*) The MBT'$_{5ME}$ vs. temperature in the culture of strain Ellin6076 (red line) together with the MBT'$_{5ME}$ in the global soil database (gray line; De Jonge et al., 2014). The data at 30 °C and 35 °C are excluded from the linear regression. (*B*) The CBT$_{5ME}$ vs. pH in the culture of strain Ellin6076 (blue line) and the global soil database (gray line; De Jonge et al., 2014). The shaded area and dash lines show 95% confidence interval and 95% prediction interval of the linear regression, respectively. (*C*) The comparison of MBT'$_{5ME}$ and CBT$_{5ME}$ values between oxygen limitation and aerobic condition. Each biological replicate is displayed and lines represent the mean values.